FAILURE MECHANICS OF MULTIPLE-SEAM MINING INTERACTIONS

By R. Karl Zipf, Jr., Ph.D., P.E.[1]

ABSTRACT

Multiple-seam mining interactions caused by full-extraction mining, whether due to undermining or overmining, frequently involve tensile failure of the affected mine roof. The adverse ground control conditions may prevent mining for both safety and economic reasons. Prior research has identified the geometric, geologic, and mining factors controlling multiple-seam mining interactions. This numerical study examines the mechanics of these interactions using a modeling procedure that (1) incorporates the essential constitutive behavior of the rock, such as strain-softening of the intact rock and shear and tensile failure along bedding planes, and (2) captures the geologic variability of the rock, especially the layering of weak and strong rocks and weak bedding planes.

Specifically, the numerical study considered the effect of vertical stress, interburden thickness, and the immediate roof quality of the affected seam in both undermining and overmining situations. The models show that for overburden-to-interburden (OB/IB) thickness ratios of less than 5, interactions do not occur and that for OB/IB more than 50, extreme interaction is a certainty. In between, the possibility of an interaction was found to depend on gob width-to-interburden thickness ratio, site-specific geology, and horizontal stress to rock strength ratio, in addition to the OB/IB ratio. The models also showed that horizontal stress was profoundly altered well above or below a full-extraction area and that these changes are likely to influence the success or failure of multiple-seam mining. The role of horizontal stress in multiple-seam mining interactions has received little attention in prior investigations.

Four factors control the mechanics of multiple-seam mining interactions:

1. Vertical stress concentration;
2. Horizontal stress concentration;
3. Stress redirection; and
4. Bedding plane slip bands.

A combination of vertical and horizontal stress increase and high-stress gradients in the vicinity of full-extraction areas reorients principal stresses into a very unfavorable direction. This seemingly small stress reorientation has a profoundly adverse effect on bedded rock.

[1]Senior research mining engineer, Pittsburgh Research Laboratory, National Institute for Occupational Safety and Health, Pittsburgh, PA.

INTRODUCTION

Most underground coal mines face multiple-seam mining situations with the potential for interactions that can pose challenging ground control conditions. Knowing the location of prior mining, planning engineers may seek to access and mine new reserves above or below old workings. Two common questions arise:

1. Will workings above or below cause excessive stresses in the proposed workings that lead to difficult ground control conditions?
2. Will subsidence from workings below cause ruinous ground control conditions in the upper seam?

In addition to ground control issues, multiple-seam mining interactions can create other safety issues. For example, an interaction can produce pathways for air, gas, or water migration that can cause spontaneous combustion and inundation hazards.

Whether an adverse multiple-seam mining interaction occurs or not depends on numerous factors that are well documented by many ground control experts [Chekan and Listak 1993, 1994; Haycocks and Zhou 1990; Hill 1995; Hladysz 1985; Hsiung and Peng 1987a,b]. These include:

1. *Mining geometry* – overburden depth, interburden thickness, and seam thicknesses;
2. *Mine design* – layout, sequence, and percent extraction; and
3. *Geology* – immediate roof rock quality and interburden rock strength.

Combination of these factors may lead to various degrees of multiple-seam mining interaction ranging from none to additional ground support required to abandonment of an area.

The ground control research program at the National Institute for Occupational Safety and Health (NIOSH) is seeking to reduce ground control failures resulting from multiple-seam mining interactions through the development of design-based control technology. This study reexamines the failure mechanics of multiple-seam mining interactions using a new numerical modeling approach under development at NIOSH. In this approach, numerical models are created with sufficient geologic detail and proper constitutive behavior. With these two conditions met, numerical models can predict the behavior of the rock mass and indicate whether an adverse multiple-seam mining interaction might occur.

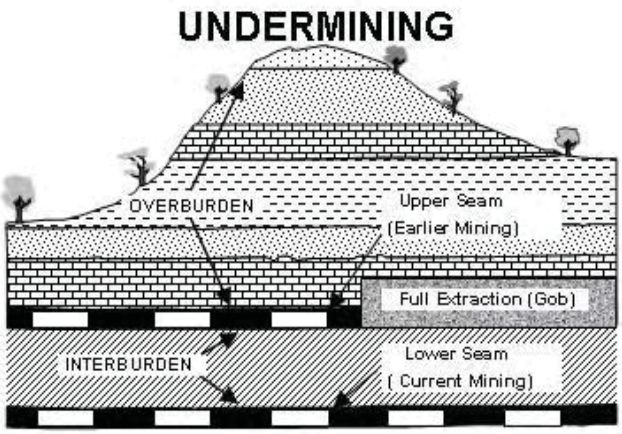

Figure 1A.—In undermining, the upper seam is mined first and abandoned, followed by lower-seam mining.

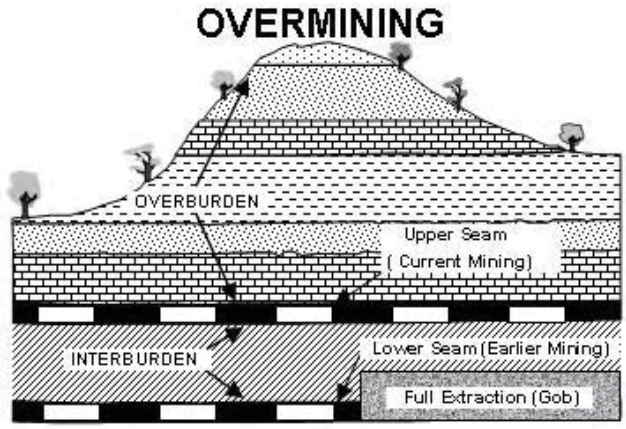

Figure 1B.—In overmining, the lower seam is mined first and abandoned, followed by upper-seam mining. The upper seam is fully subsided prior to its mining.

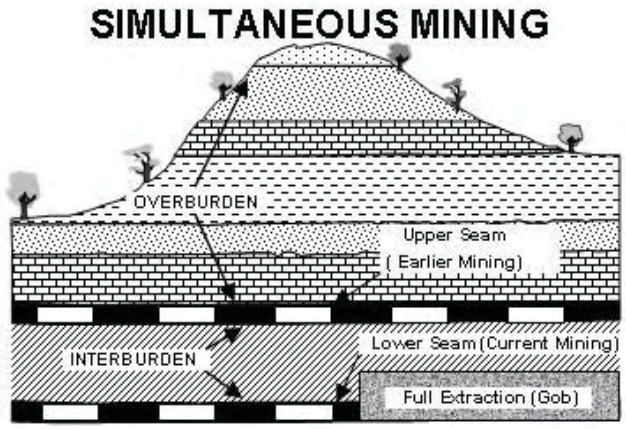

Figure 1C.—In simultaneous mining, the upper seam is developed first, followed by lower-seam mining. Full-extraction mining of the lower seam subsides existing upper-seam workings.

This study examines three fundamental types of multiple-seam interaction:

1. *Undermining* (Figure 1A): This situation represents classic top-down multiple-seam mining. The upper seam is mined first and abandoned prior to mining the lower seam. Gob-solid boundaries, barrier pillars, pillar remnants, or other structures left over from full-extraction mining in the upper seam may cause adverse stress concentrations in the lower seam.
2. *Overmining* (Figure 1B): This situation represents classic bottom-up multiple-seam mining. Full-extraction mining in the lower seam causes the upper seam to fully subside prior to its development. In addition to stress concentrations due to pillar remnants or gob-solid boundaries in the lower seam, the upper seam and surrounding rock may suffer damage from subsidence-induced displacement and fracture.
3. *Simultaneous mining* (Figure 1C): This situation implies that both seams are active simultaneously. In the worst case, workings are developed in the upper seam followed by full-extraction mining in the lower seam. Subsidence of the upper seam occurs after the lower-seam workings are extracted.

NIOSH INPUT PARAMETERS FOR NUMERICAL MODELING

Ground control researchers at NIOSH follow a philosophy developed by Gale [Gale and Tarrant 1997; Gale 2004; Gale et al. 2004] of "letting the rocks tell us their behavior." Numerical models that are constructed with sufficient geologic detail and proper constitutive behavior can predict response of the rock mass, including deformation, stress redistribution, failure modes, and support requirements. For general modeling of rock behavior in coal mine ground control, Itasca's FLAC program [Itasca Consulting Group 2000] contains many useful features, in particular, the SU constitutive model. SU stands for the strain-softening, ubiquitous joint model and is ideal for simulating laminated coal measure rocks. In essence, this constitutive model allows for strain-softening behavior of the rock matrix and/or failure along a predefined weakness plane (in this case bedding planes). Failure through the rock matrix or along a bedding plane can occur via shear or tension, and the dominant failure mode can change at any time. Conveniently, the "state" variable within FLAC tracks the failure mode in each model element as either shear or tensile failure through the rock matrix or along a bedding plane.

The SU constitutive model requires four major input parameters, namely, cohesion, friction angle, dilation angle, and tensile strength for both the rock matrix and the

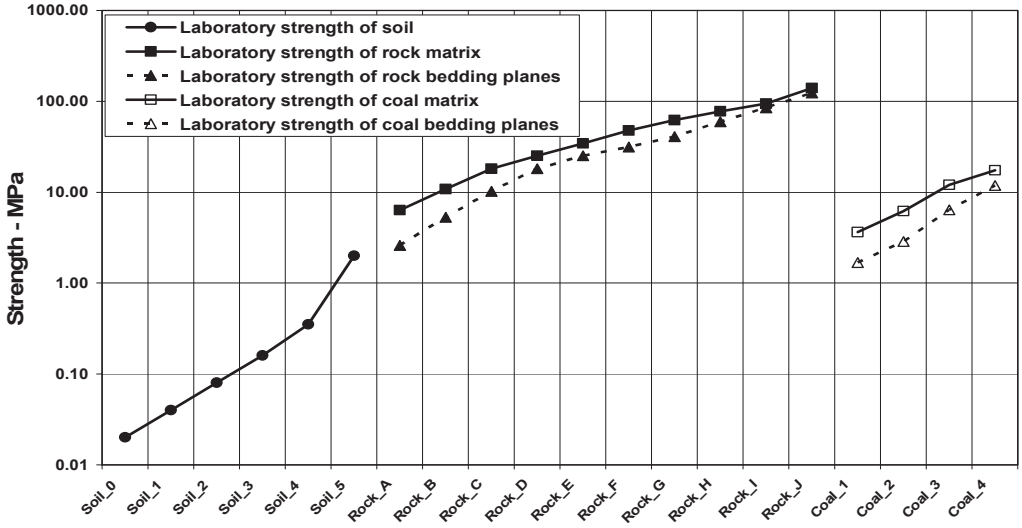

Figure 2.—Laboratory-scale strength of matrix and bedding planes for suite of "numerical rocks."

bedding planes. Each of these parameters begins at some peak value and decreases to a residual value as postfailure strain increases. It is this decrease in parameter value with postfailure strain that gives rise to strain-softening behavior of both the rock matrix and the weakness planes. FLAC permits an infinite combination of these requisite input parameters; however, in order to facilitate rational numerical modeling, NIOSH researchers created an organized suite of material input parameters. Figure 2 summarizes the names for this suite of "numerical rocks" and the corresponding values for the unconfined compressive strength (UCS) of the rock matrix and the strength of the bedding planes.

The strength values shown in Figure 2 are laboratory-scale values determined from standard UCS tests. Alternatively, the point load test provides excellent, economic estimates of the UCS. These UCS values require scaling to reduce the laboratory values to the field values needed by the numerical model. Following the lead of Gale and Tarrant [1997], laboratory values of UCS are reduced by 0.56 universally.

The material suite shown in Figure 2 includes very weak soils and claylike materials with a UCS of 0.02 MPa and weak, medium, and finally strong rocks with a UCS of about 150 MPa. Also included is coal, which ranges from the most friable with a UCS of 2 MPa to a strong coal with a UCS of 12 MPa. The soil material models are isotropic, that is, the soil matrix properties are the same as those for the horizontal weakness plane. However, the rock models exhibit anisotropy since the strength along bedding planes is less than the UCS of the rock matrix. Following results of point load tests by Molinda and Mark [1996], weak rocks are the most anisotropic with the strength along bedding planes about 50% of the rock matrix UCS, while stronger rocks have less anisotropy with the strength along bedding planes about 90% of the rock matrix. The coal models have a similar trend in strength anisotropy, with the stronger coal less anisotropic than the weaker coal.

Note that in proposing this suite of numerical rocks, the UCS of the rock matrix is independent from the strength of the bedding planes. In the absence of specific data, the user will usually specify the rock matrix and bedding plane strength as a pair, with strength ratio similar to that noted by Molinda and Mark [1996] for an extensive database of axial and diametral point load tests. However, the strength values for the rock matrix and bedding planes are independent in the material property suite, and the user can specify any value for the bedding plane strength up to that of the rock matrix UCS.

Also note that the material model suite has a relation to the unit ratings in the Coal Mine Roof Rating (CMRR) system. Mark et al. [2002] proposed that the CMRR unit rating for a coal measure rock layer is comprised of a UCS rating for the rock matrix strength and a discontinuity rating for the bedding plane strength. The UCS rating ranges from 5 to 30 points for a rock matrix strength ranging from 0 to 138 MPa as determined from axial point load tests. Similarly, the discontinuity rating ranges from 25 to 60 for a bedding plane strength ranging from about 6 to 52 MPa as determined from diametral point load tests. The proposed material property suite correlates to CMRR unit ratings from 30 to 90 and represents the range from the weakest to the strongest coal measure rocks. Figure 3 shows these relations. Given CMRR unit ratings from core logging, the relations shown in Figure 3 provide approximate material choices for input to numerical models.

The material model suite and UCS values shown in Figure 2 imply a range of cohesion and friction angle values for the rock matrix and bedding planes. Based on a Mohr-Coulomb strength model, the UCS of a rock depends on cohesion and friction angle as—

$$UCS = \frac{2\,c\cos\phi}{1-\sin\phi} \qquad (1)$$

where c is the cohesion and ϕ is the friction angle. Friction angle for the different materials in the suite is assumed to vary, as shown in Figure 4. Soil and claylike materials have friction angles of 21°, while progressively stronger rocks have friction angles up to 36°. This assumption for friction angle along with Equation 1 implies the values for peak cohesion shown in Figure 5. Thus, the UCS of the rock matrix and the bedding plane strength provide two of the four major input parameters to the SU constitutive model in FLAC.

Other major assumptions within this material model suite are as follows:

1. Moduli for the materials range from 1 to 20 GPa, as shown in Figure 6. Weaker materials have a lower modulus, while stronger materials have a higher modulus. The ratio of modulus to UCS of the rock matrix varies from about 10,000 for the weakest to about 100 for the strongest materials.
2. Cohesion decreases from its peak value given in Figure 5 to a residual value of 10% of peak over 5 millistrain of postfailure strain.
3. Friction angle remains constant at the values shown in Figure 4, even in the postfailure regime.
4. Tensile strength is equal to cohesion for the soil materials and decreases to 0 over 1 millistrain of postfailure strain.
5. Tensile strength ranges from about 10% of UCS for the weakest rocks to about 2% of UCS for the

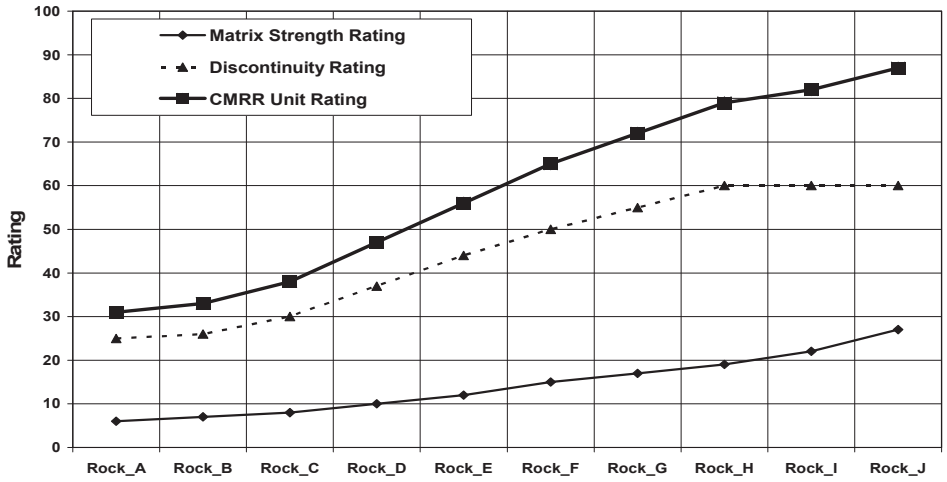

Figure 3.—Correlation of "numerical rocks" to unit ratings of the Coal Mine Roof Rating (CMRR) system. Weak rocks have a CMRR unit rating from 30 to 45; moderate rocks, from 45 to 60; and strong rocks, from 60 to 85.

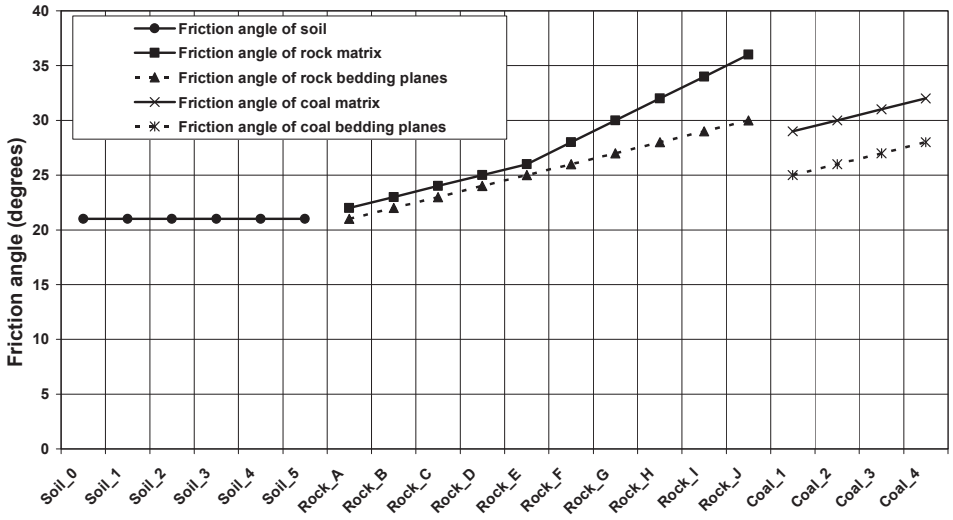

Figure 4.—Friction angle for matrix and bedding planes in suite of "numerical rocks."

strongest rocks. It also decreases to 0 over 1 millistrain of postfailure strain.

6. Dilation angle is initially 10° and decreases to 0° over 5 millistrain of postfailure strain.

This suite of material models provides a convenient method for the modeler to go from a geologic log to a numerical model in a rational, systematic, and efficient manner. Table 1 illustrates this process and shows the level of detail needed for geologic logging. On the left is a typical core log with geologic description. Geologic features at a scale as small as 50 mm are typically recorded for this log. Of particular importance to note are soft clay layers or major bedding planes with weak infilling. In the middle of

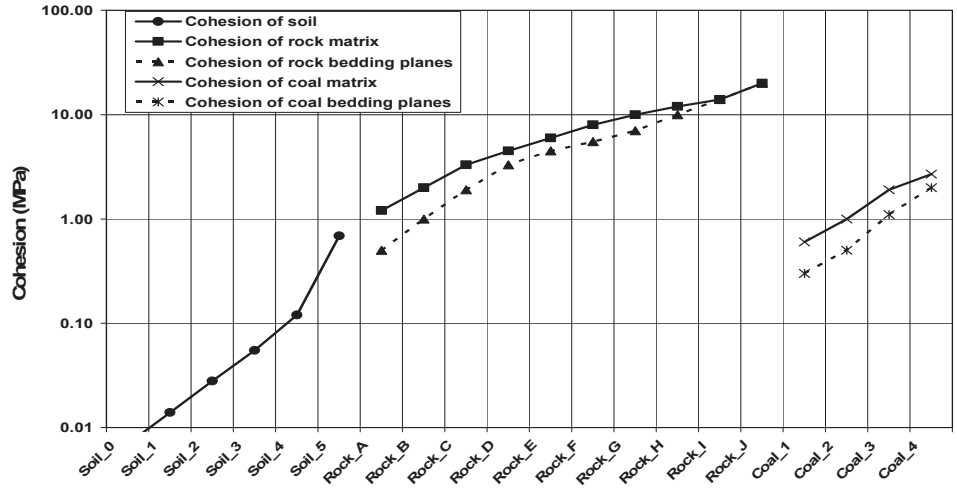

Figure 5.—Cohesion of matrix and bedding planes in suite of "numerical rocks."

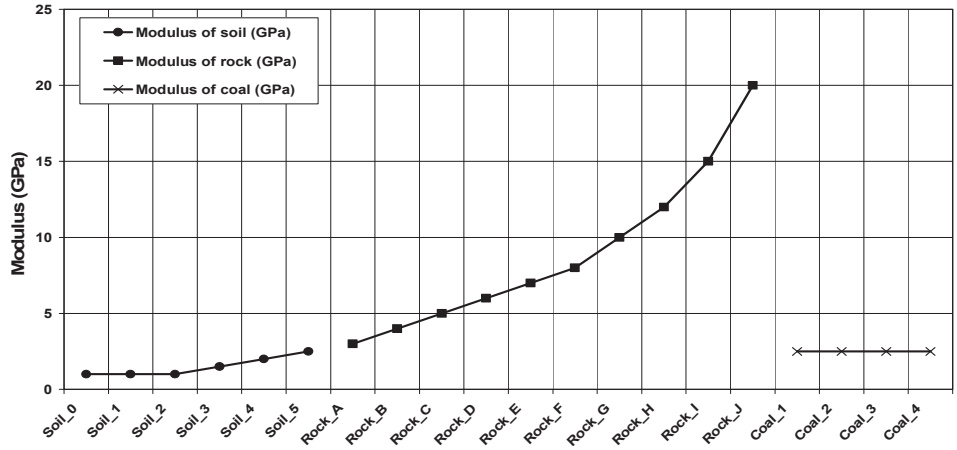

Figure 6.—Modulus of matrix in suite of "numerical rocks."

Table 1.—Going from core log to numerical model input parameters

Stratigraphic column		UCS from axial point load tests (MPa)	UCS from diametral point load tests (MPa)	Rock matrix strength code	Bedding plane strength code
Rock type	Thickness (m)				
Strong sandstone	2.4	90	80	Rock_I	Rock_I
Siltstone (stackrock)	1.2	35	5	Rock_E	Rock_B
Black shale	1.9	10	5	Rock_B	Rock_B
Soft clay	0.05	0.2	0.2	Soil_3	Soil_3
Gray shale	1.8	25	10	Rock_D	Rock_C

Table 1 are UCS estimates for each unit from axial and diametral point load tests. Finally, on the right of the table are property codes for generating input parameters to numerical models using the material model suite presented herein. The modeling approach described has been verified against detailed monitoring of a coal mine entry done by Oyler et al. [2004].

MULTIPLE-SEAM MINING INTERACTION MODEL CONSTRUCTION

Using the material input parameters described above, models were created for the three interaction types, as shown in Figure 7. All models examine mining either above or below a gob-solid boundary, which is representative of most interactions, including mining above or below pillar remnants or barrier pillars. In undermining, a longwall is mined first in the upper seam followed by room-and-pillar development in the lower seam. In overmining, a longwall is mined first in the lower seam followed by room-and-pillar development in the upper seam. In simultaneous mining, room-and-pillar development is done in the upper seam followed by longwall mining in the lower seam. These model types enable detailed examination of the failure mechanics of coal mine entries subject to multiple-seam mining interactions, with the focus on the transition zone either above or below the gob-solid boundary.

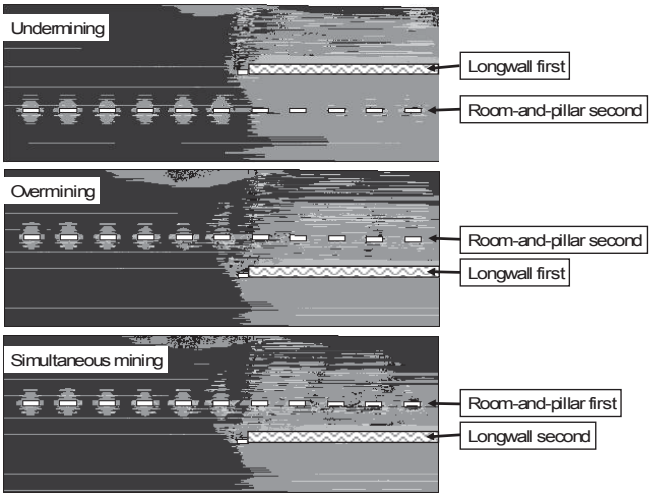

Figure 7.—Multiple-seam mining interaction models for three interaction types. In undermining, a longwall is mined in the upper seam first, followed by room-and-pillar mining in the lower seam. In overmining, a longwall is mined in the lower seam first and the upper seam subsides fully, followed by room-and-pillar mining in the upper seam. In simultaneous mining, the upper seam is developed first and then a longwall mines the lower seam, causing subsidence of the existing workings in the upper seam. Dark shading indicates intact rock; lighter shading indicates matrix failure or slip along bedding planes.

The models consider a slice of the rock mass 160 m wide and up to 75 m high. Each model contains 450 elements along the width and up to 515 elements along the height. Coal seam thickness is 2 m, entry width is 6 m, and entry height is also 2 m. The thickness of each geologic layer is about 0.15 m on average and ranges from 0.05 to 0.25 m. Most of the rock mass layers are assigned properties corresponding to CMRR unit ratings of 45 to 60, which is equivalent to a moderate strength rock mass. However, as discussed later, the immediate roof of the affected seam is considered separately. The stratigraphy used in the model is extracted from a detailed core log similar to that shown in Table 1. Weak, moderate, and strong sections from this log were assembled as needed. While the models are artificial, they have a basis on a real geologic log.

Following recent work on horizontal stress by Dolinar [2003], an average horizontal stress of 10 MPa is applied to the model via the equivalent horizontal strain. Thus, horizontal stress varies according to the relative stiffness of each geologic layer. Stiffer layers have higher horizontal stress than softer layers. Vertical stress is applied at the top of the model to simulate cover load.

The full-extraction area is approximated as a strain-hardening material using the DY, or double yield, constitutive model that can simulate irreversible compaction. Thus, a gob layer replaces the mined coal seam over a height of three times the coal seam thickness. This approximation leads to subsidence over the full-extraction area of about 50% of the seam thickness.

As shown in Figure 8, each model type examined the effect of three factors on the mechanics of multiple-seam mining interaction. Each variable in the matrix has just two values. Vertical stress is either 3 MPa or 9 MPa, which implies an overburden depth of 120 m (shallow) or 360 m (deep). Interburden thickness is either close (7 m) or intermediate (24 m). Finally, the immediate roof quality is either weak (CMRR unit rating of 30–45) or strong (CMRR unit rating of 60–80).

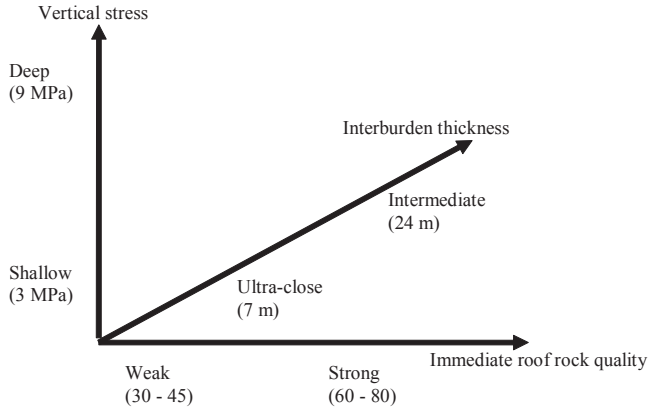

Figure 8.—Three variables for numerical modeling matrix of multiple-seam mining interactions.

Preliminary analysis of case history data presented by Ellenberger et al. [2003] suggests that multiple-seam mining interactions are possible when the OB/IB thickness ratio exceeds 7 for both undermining and overmining cases. By implication, this modeling matrix considers three OB/IB ratio values, namely, 5 where no interaction is expected, about 15–17 where an interaction is possible, and 51 where an interaction is likely.

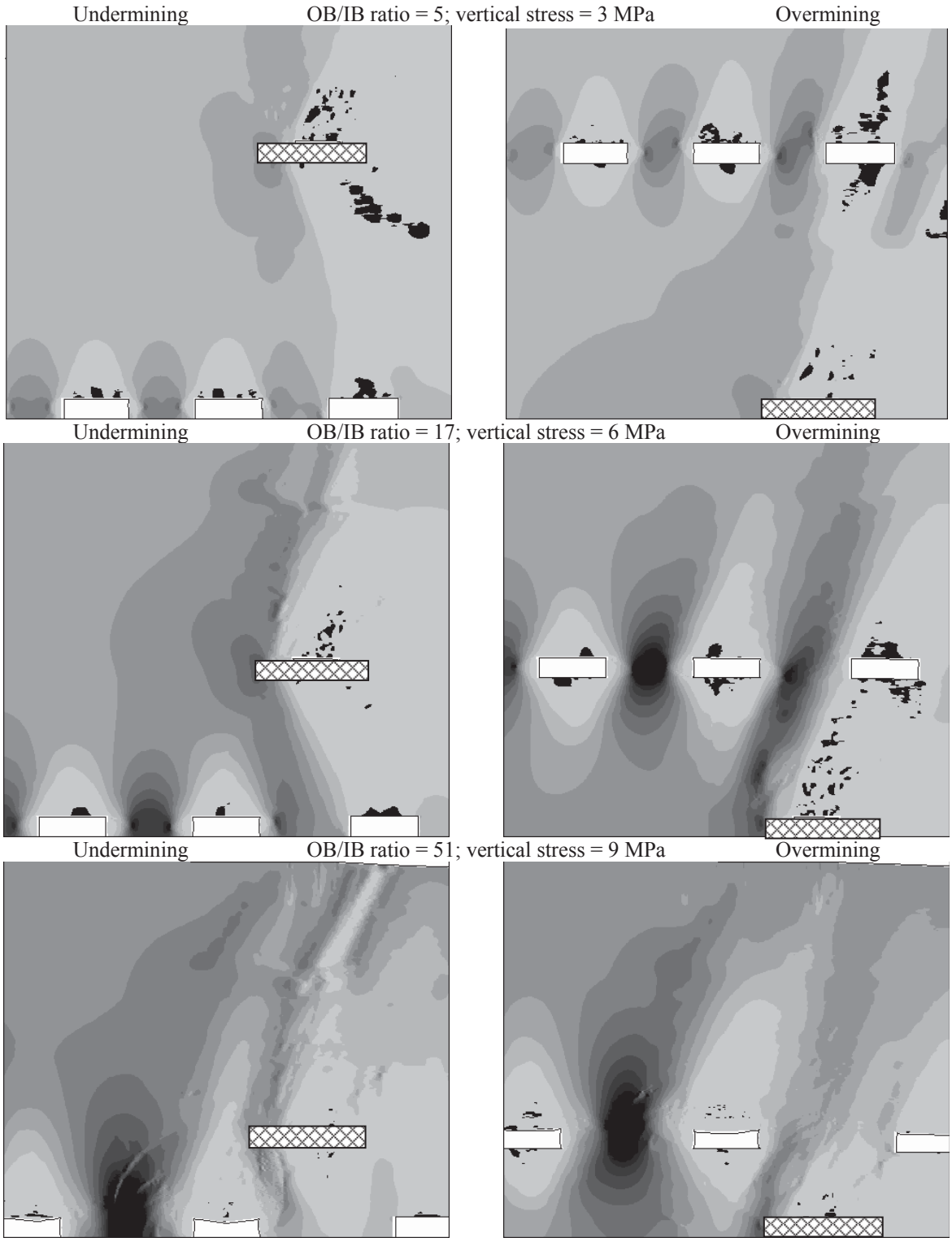

Figure 9.—Vertical stress comparison. Dark shading indicates high stress; light shading indicates low stress. Applied horizontal stress is 10 MPa. Hatching indicates longwall.

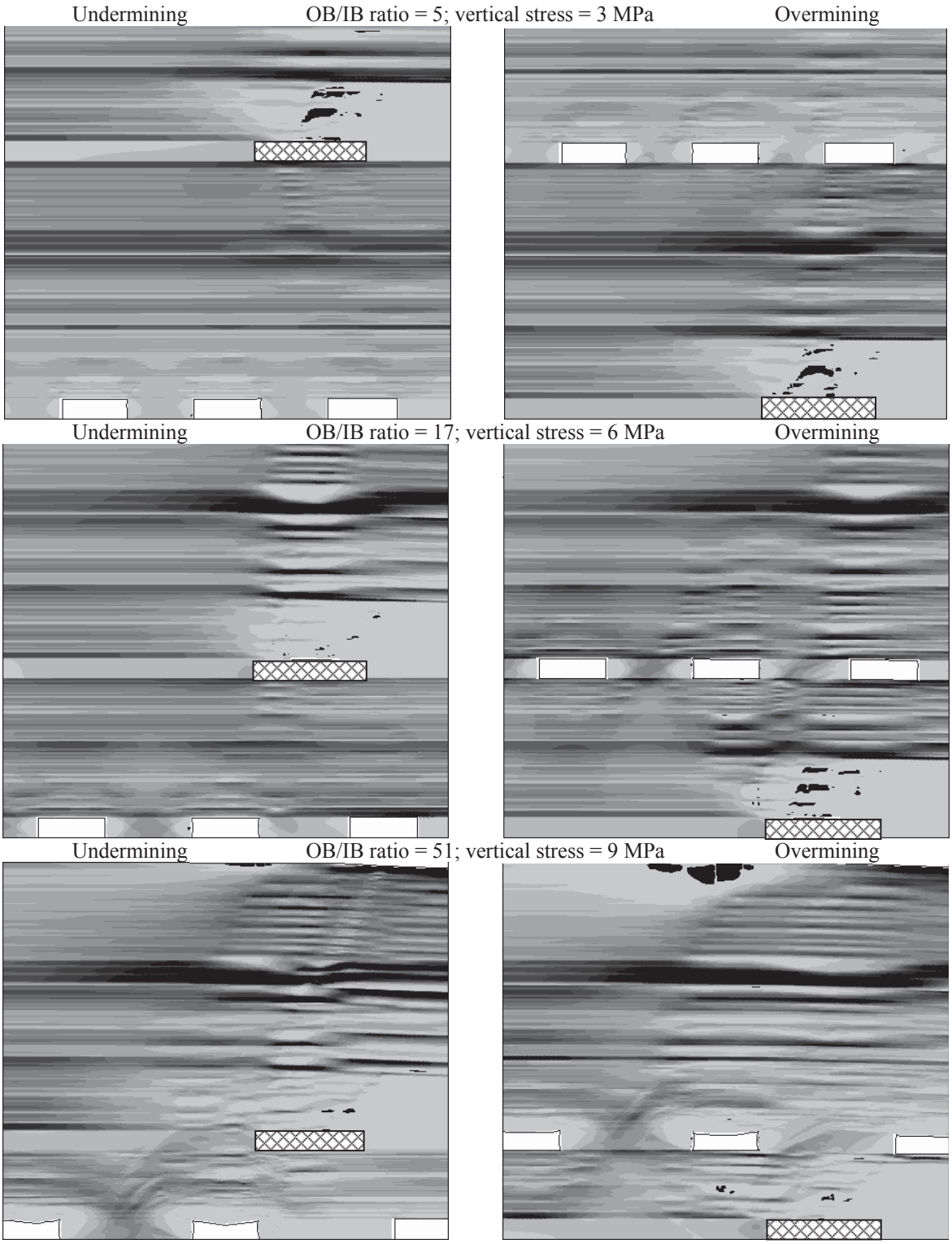

Figure 10.—Horizontal stress comparison. Dark shading indicates high stress; light shading indicates low stress. Applied horizontal stress is 10 MPa. Hatching indicates longwall.

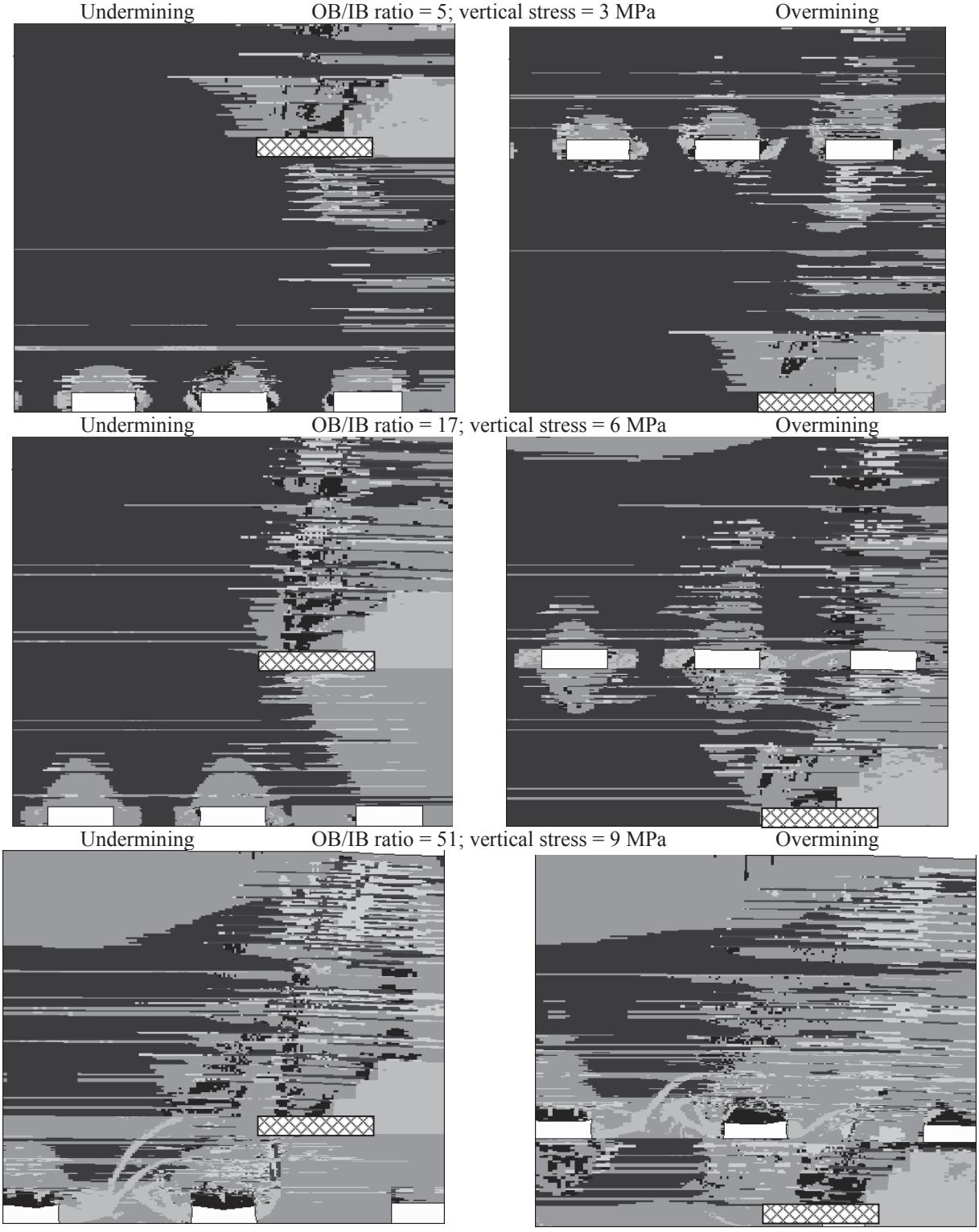

Figure 11.—Failure state comparison. Dark shading indicates intact rock. Lighter shading indicates matrix failure or slip along bedding planes. Applied horizontal stress is 10 MPa. Hatching indicates longwall.

COMPARISON OF MULTIPLE-SEAM MINING INTERACTION MODELS

Figures 9–11 compare vertical stress, horizontal stress, ,and failure state images, respectively, for the undermining and overmining type of multiple-seam mining interactions. The top image in each figure is for an OB/IB ratio of 5, where no multiple-seam mining interaction is expected. Vertical stress is low (3 MPa), and immediate roof rock quality is weak. These models lie near the lower left corner of the matrix shown in Figure 8. In the middle image, the OB/IB ratio is 17, so a multiple-seam mining interaction is possible. Vertical stress is medium (6 MPa), and immediate roof rock quality is medium. These models lie at the center of the matrix. Finally, the lower image is for an OB/IB ratio of 51, where an adverse multiple-seam mining interaction is highly likely. Vertical stress is high (9 MPa), and immediate roof rock quality is weak. These models lie at the upper left corner of the matrix shown in Figure 8.

The following general observations are noted.

1. Vertical stress concentrations occur in a narrow band above and below the gob-solid boundary. This band is inclined about 20° toward the gob both above and below the full-extraction seam. A vertical stress shadow occurs above and below the gob, and it diminishes slowly about 50 m from the gob-solid boundary where the gob has fully reconsolidated.
2. Full-extraction mining produces horizontal stress changes several tens of meters above and below the mined area. The horizontal stress changes occur much farther above and below the mined area than do the associated vertical stress changes laterally away from that mined area. The horizontal stress concentrations may in turn induce rock failure in select geologic layers well above or below the mined area that can further amplify horizontal stress concentrations in nearby layers.
3. Bedding plane slip and tensile failure through the rock matrix occur in a narrow band directly above and below the gob-solid boundary. This band is more extensive above the extracted seam; however, it also extends a considerable distance below it.
4. For coal mine entries in moderate strength immediate roof rock (CMRR unit rating of 45– 60), the extent of rock failure through bedding plane shear or tensile failure of the rock matrix is about 1 times the entry width.

With respect to undermining, the following additional observations are noted.

1. A zone of vertical stress relief occurs under the full-extraction mining area beginning past the gob-solid boundary and extending several tens of meters under the gob. This zone is well understood and correlates well with the best practice of offsetting gate roads under the gob for optimal stability in multiple-seam mining.
2. There is increased bedding plane slip in entries close to directly below a gob-solid boundary. The additional failure is slight and should not correspond to significant additional support requirements.
3. There is a small increase in the amount of pillar failure in the zone below the gob-solid boundary. This increase might correspond to additional pillar spalling and nothing more. As before, the additional pillar failure is slight and not indicative of severe ground control conditions.

With respect to overmining, the following additional observations are noted.

1. A significant increase in bedding plane slip and tensile failure occurs in the interburden and immediate roof rock along with pillar failure in the upper coal seam within a narrow band above the gob-solid boundary. This observation correlates with known decreases in entry and pillar stability in the transition zone above a gob-solid boundary [Rigsby et al. 2003].
2. There is no apparent increase in bedding plane slip or additional tensile failure in the immediate roof above coal mine entries developed in a coal seam that has subsided due to prior mining below. This numerical observation also correlates well with the good stability generally observed in entries driven in fully subsided coal seams. The failure zone induced by entry development in subsided ground is not substantially different from that of an entry in completely undisturbed ground.

With respect to simultaneous mining, the following additional observations are noted without showing the associated models.

1. The horizontal and vertical stress distribution is virtually identical to that shown for simple overmining.
2. The failure mode situation is completely different. When the longwall is created in the lower seam, calculations show a wave of tensile failure that propagates upward through the rock mass and completely envelopes the developed entries within this failure zone. Thus, these entries are likely to experience deteriorating ground control

conditions. This situation is completely different from the prior situation of entry development in a previously subsided coal seam.

Tables 2 and 3 compare notes about the undermining and overmining models within the modeling matrix described by Figure 8. These tables compare conditions around an entry not subject to any multiple-seam mining interaction to an entry subject to full interaction in the area directly above or below a gob-solid boundary. The comparisons examine relative changes on vertical stress, horizontal stress, and failure mode as the OB/IB ratio increases from 5 to 51. Figures 9–11 help illustrate this semi-quantitative comparison of changes in relative stress and failure zone size. As expected, the tables show interesting trends as the OB/IB ratio increases from 5, where no interaction is expected, to over 50, where a serious multiple-seam mining interaction is expected.

Vertical Stress Comparison

In Tables 2 and 3, the vertical stress comparison documents stress changes in pillars above or below a gob-solid boundary compared to a pillar far from the interaction area. As indicated in Table 2, when undermining with a low OB/IB ratio of 5 (Figure 9, top), there is little change in vertical stress within pillars near the gob-solid boundary compared to pillars far away, no matter whether the immediate roof rock is weak or strong. As the OB/IB ratio increases to 17 or 51 (Figure 9, middle and bottom), the relative vertical stress concentration increases significantly. Again, the strength of the immediate roof rock makes little difference in this increase.

Table 2.—Comparison of undermining models

OB/IB ratio	Weak immediate roof rock	Strong immediate roof rock
Vertical stress comparison		
5	Little change	Little change
15–17	Increases about 25% to 50%	Increases about 50%
51	Increase more than 50%	Increase more than 50%
Horizontal stress comparison		
5	Increases less than 10%	Increases about 25%
15–17	Decreases due to failure	Increases about 50%
51	Decreases due to failure	Increases more than 50%
Failure size comparison (remote entry and under gob-solid boundary)		
5	Slight increase in size	0.1 × entry width and no increase in size
15–17	0.5 to 1 × entry width to 1 to 1.5 × entry width	0.1 to 1 × entry width to 0.25 to 1 × entry width
51	1 × entry width to more than 2 × entry width	1 × entry width to 1.5 × entry width

Table 3.—Comparison of overmining models

OB/IB ratio	Weak immediate roof rock	Strong immediate roof rock
Vertical stress comparison		
5	Increases about 20%	Increases about 20%
15–17	Increases about 25% to 50%	Increases about 25% to 50%
51	Increase more than 50%	Increase more than 50%
Horizontal stress comparison		
5	Increases about 10%	Increases about 50%
15–17	Small increases and decreases due to failure	Increases about 50%
51	Decreases due to failure	Increases more than 50% and decreases due to failure
Failure size comparison (remote entry and under gob-solid boundary)		
5	0.3 × entry width to 1 × entry width	0.1 × entry width and no increase in size
15–17	0.5 to 1 × entry width to 1 to 1.5 × entry width	0.1 to 1 × entry width to 0.1 to 1.5 × entry width
51	1.5 × entry width to more than 2 × entry width	1 × entry width to 1.5 × entry width

When overmining, it seems there is more upward transmission of vertical stress concentration. As indicated in Table 3 and shown in Figure 9, at low OB/IB ratio, a significant relative increase in vertical stress does occur. At higher OB/IB ratios of 17 and 51, the relative vertical stress concentration increases, but it is not substantially different from that seen with undermining. Subsidence and the extent of the broken gob above the seam horizon may account for the difference at low OB/IB ratio. As with undermining, the strength of the immediate roof rock makes little difference with regard to the magnitude of the relative vertical stress changes in the pillars.

The overburden and interburden rock in all models is medium strength, with CMRR ranging from 45 to 60. Changing the physical nature of the interburden rock will change the vertical stress distribution; however, it will not change the relative vertical stress changes as noted in this comparison.

Horizontal Stress Comparison

The horizontal stress comparison documents stress changes in the immediate roof rock of an entry above or below a gob-solid boundary compared to an entry far from the expected interaction area. As shown in Tables 2 and 3 and Figure 10, at a low OB/IB ratio of 5, where no interaction is expected, horizontal stress does increase slightly above the background level and that increase depends on the strength of the immediate roof rock. A weak immediate roof rock sees a small increase, while strong immediate roof rock sees a much larger increase in horizontal stress. The relative increase in horizontal stress is more pronounced in overmining compared to

undermining for reasons of subsidence and gob formation noted earlier.

As the OB/IB ratio increases, the change in horizontal stress from background depends on the strength of the immediate roof rock. With weak roof, horizontal stress decreases in the interaction area when the immediate roof rock fails and stress is distributed elsewhere. With stronger roof, horizontal stress in the interaction area can increase dramatically over background (50% or more). However, at sufficiently high OB/IB ratio, even strong immediate roof rock can be made to fail in the interaction zone, with a resulting decrease in horizontal stress. Table 3 for overmining shows this possibility.

The role of horizontal stress is crucial for further understanding of multiple-seam mining interaction. As seen in Figure 10, a full-extraction area induces horizontal stress changes many tens of meters above and below the mined seam. The magnitude of these changes depends on several factors, namely, OB/IB ratio, site-specific geology, the ratio of extraction area width to interburden thickness, and the ratio of horizontal stress to immediate roof rock strength.

The OB/IB ratio affects the geometry and the vertical stress level of the particular situation. Closer proximity of the affected seam to undermining and overmining has the expected effect on horizontal stress magnitude. With respect to geology, the major variable is the percentage of strong rock in the interburden and where that strong rock is located relative to the affected roof. A suitably placed strong bed can shield the immediate roof rock of a seam from adverse multiple-seam mining interaction. The ratio of extraction area to interburden thickness is another geometry factor that controls how far above or below a full-extraction area the horizontal stress might change. There are limits on this ratio that depend on whether the full-extraction area exceeds the "critical width" at which maximum subsidence is achieved and vertical stress in the middle of the full-extraction area returns to in situ value. Finally, the ratio of applied horizontal stress (in situ plus induced) to the strength of the immediate roof rock controls the degree of multiple-seam mining interaction. A higher ratio due to either high horizontal stress or low immediate roof rock strength increases the chance of an adverse interaction. Horizontal stress has been found to be a major factor in many ground control problems, especially in the Eastern United States [Mark and Mucho [1994].

Failure Size Comparison

The failure size comparison documents the extent of rock matrix or bedding plane failure in either shear or tension within the immediate roof of the affected seam. The entry itself induces a failure zone in the immediate roof whose extent depends on overburden depth and immediate roof rock quality. This comparison notes how much additional failure occurs due to nearby multiple-seam mining. Failure extent is gauged relative to the entry width.

When undermining at low OB/IB ratio (Table 2), the overlying gob-solid boundary is far away, and it induces little additional failure about an entry in the potential interaction area (Figure 9). For high OB/IB ratio, the overlying gob-solid boundary is close, and the size of the failure zone grows by more than a factor of 2 in weak rock, as shown in Figure 11. Strong rocks show a similar trend as indicated in Table 2. At low OB/IB ratio, the interaction is negligible, while at high OB/IB ratio, the added interaction is severe even with strong immediate roof rock.

At intermediate values of OB/IB ratio, induced changes in the failure zone extent due to multiple-seam interaction can vary greatly. For one case in weak roof, it changes from ½ to 1 times the entry width, while in another case, it changes from 1 to 1½ times the entry width. With stronger rocks, the variability is even more pronounced. In one case, failure zone size changes from one-tenth to one-fourth times the entry width, and in another it remained the same size at 1 times entry width.

Failure zone size in the overmining models (Table 3) showed a similar trend. At low OB/IB ratio in weak rock, failure size is somewhat larger initially and grows more than in the undermining models, while in stronger rock there is no difference. At high OB/IB ratio, failure size grows significantly in both weak and strong rock, which is indicative of a substantial multiple-seam mining interaction. At intermediate OB/IB ratio, failure zone extent and its changes vary greatly as in the undermining models.

The observed changes in failure zone size reflect similar trends as seen with horizontal stress. For an OB/IB ratio less than 5, the chance of a multiple-seam mining interaction is very low, even under a weak immediate roof rock. An adverse interaction is expected for a high OB/IB ratio greater than 50, even under strong immediate roof rock. For an intermediate OB/IB ratio of around 17, the chance of an adverse interaction depends on the vagaries of the interburden rock, in particular site-specific geology and the ratio of horizontal stress to rock strength, and geometric factors such as the ratio of full-extraction width to interburden thickness.

MECHANICAL FACTORS IN MULTIPLE-SEAM MINING INTERACTIONS

The simple modeling matrix reproduces successfully many practical observations of multiple-seam mining interactions, lending credibility to the numerical model and the NIOSH input parameters. Close inspection of the models considered here suggests four underlying factors controlling the failure mechanics of multiple-seam mining interactions:

1. Vertical stress concentration;
2. Horizontal stress concentration;
3. Stress redirection; and
4. Bedding plane slip bands.

Vertical stress concentrations (Figure 12) occur in the vicinity of gob-solid boundaries, pillar remnants, and similar structures as vertical stress is diverted around full-extraction areas. The lateral extent of these increases is indicated in Figure 12 along with stress relief areas. The degree of vertical stress concentration decreases quickly with lateral distance from this boundary. The extent of vertical stress relief above and below the full-extraction area depends on the width of that area. There is also an associated vertical stress gradient near a gob-solid boundary.

Horizontal stress concentrations (Figure 13) also develop around full-extraction areas; however, their behavior is much more complex. Horizontal stress concentration depends on both distance above and below the full-extraction area and the relative stiffness of the geologic layers. Furthermore, horizontal stress concentrations can

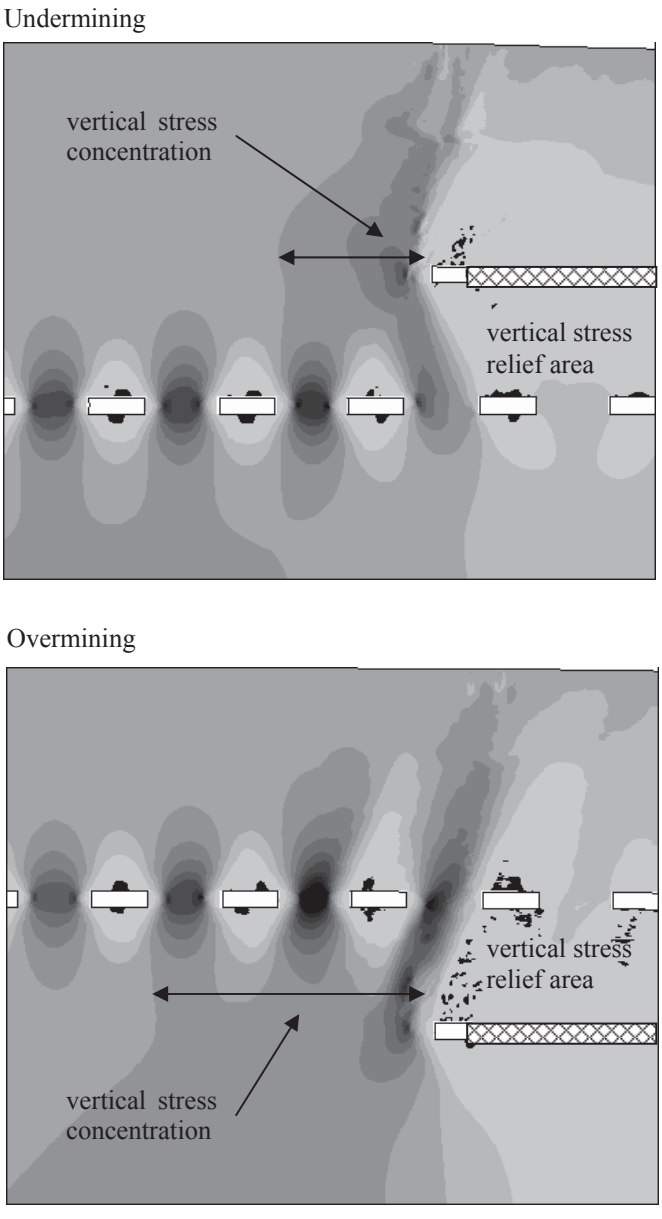

Figure 12.—Vertical stress concentration above and below gob-solid boundaries. Dark shading indicates high stress; light shading indicates low stress. Hatching indicates longwall.

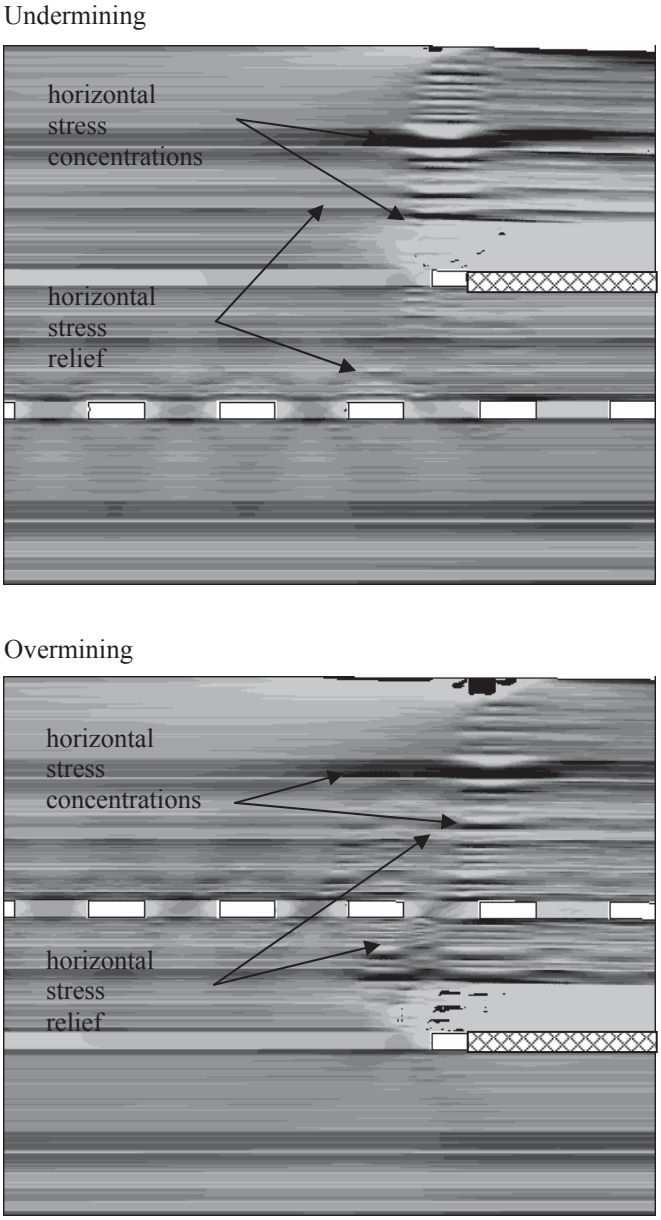

Figure 13.—Horizontal stress concentration above and below full-extraction areas. Dark shading indicates high stress; light shading indicates low stress. Hatching indicates longwall.

be expected much farther above or below a full-extraction area than vertical stress concentrations can be expected left or right of that area. Horizontal stress redistribution is seen much farther away, and it may induce failure in certain weaker layers, leading to even more horizontal stress redistribution. It seems that the effect of horizontal stress on multiple-seam mining interactions has not been explored in any prior studies. The extent of horizontal stress concentration and associated failure of select layers may explain certain cases of successful and unsuccessful multiple-seam mining in otherwise similar conditions.

The combination of vertical and horizontal stress increases in the vicinity of a full-extraction area and, in particular, stress gradients will reorient the principal stresses, as illustrated in Figure 14. This seemingly small stress reorientation has a profound effect on bedded rock. In the absence of mining, principal stresses are usually oriented parallel and perpendicular to geologic strata (Figure 14, top), which is a more favorable orientation for strength. Full-extraction mining reorients principal stresses to the weaker orientation shown in the bottom of Figure 14. Coal mine entries developed in nearby seams in this rotated stress field are much more likely to experience unfavorable ground control conditions. It is also noted without illustration that reorientation of the principal stress occurs in a fairly narrow vertical band adjacent to the gob-solid interface.

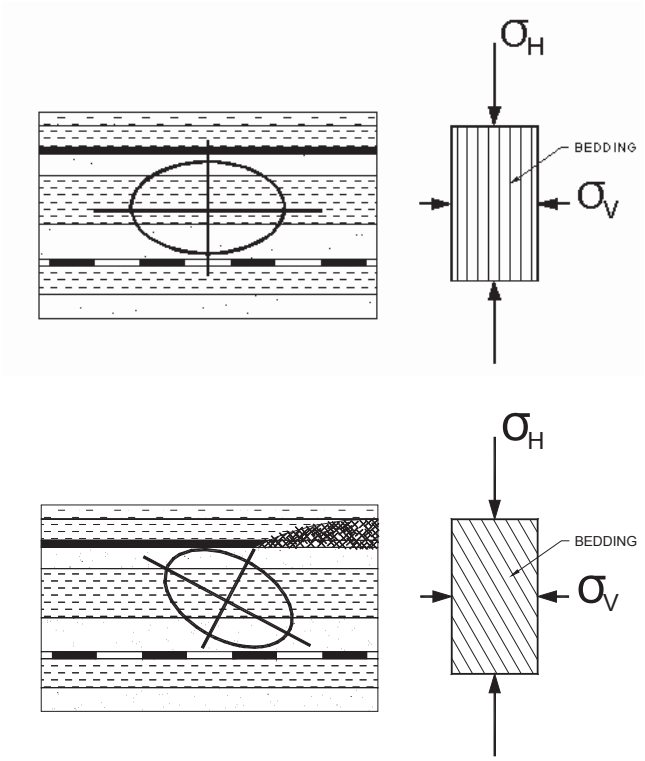

Figure 14.—Reorientation of principal stresses leads to failure due to multiple-seam mining interaction. In single-seam mining, far-field principal stresses are generally aligned parallel to the bedding planes in which a test specimen is relatively strong. If the far-field principal stresses are rotated due to nearby multiple-seam mining, the bedding planes are oriented in an unfavorable direction in which a test specimen is relatively weak.

The rotated stress field also leads to bedding plane slip in narrow, subvertical zones above and below gob-solid boundaries, as seen in the failure state plots in Figures 9–11. These zones of bedding shear are also more likely areas for unfavorable ground control conditions.

TOWARD DESIGN GUIDELINES FOR MULTIPLE-SEAM MINING

This research seeks to provide design guidelines that enable mine planning engineers to correctly assess the safety risk of an adverse multiple-seam mining interaction based on mine geometry factors, mine layout factors, and site-specific geologic conditions. Preliminary analysis of case studies by Ellenberger et al. [2003] suggested that for both undermining and overmining, when the OB/IB ratio was less than 7, there was little risk of adverse interaction. For an OB/IB ratio above 16, there was a possibility of extreme interaction; however, it became evident that other factors in addition to OB/IB also became important.

Numerical studies conducted during this research examined the effect of OB/IB ratio and the immediate roof rock quality of the affected seam on the degree of multiple-seam mining interaction. The numerical models utilized contain great geologic detail and the proper constitutive behavior and are able to capture the essential failure modes of the rock mass, in particular, shear or tensile failure through the rock matrix or along bedding planes.

The numerical models confirm aspects of the initial multiple-seam mining interaction guidelines above. When the OB/IB ratio is less than 5, the models clearly show little, if any, interaction between mining in nearby seams. When the OB/IB ratio exceeds 50, the models clearly show an extreme interaction, even with strong roof conditions in the affected seam. For the intermediate OB/IB ratios considered (15–17), the models show that an adverse interaction is possible, and they provide some insight into the controlling factors.

Numerical models show how vertical stresses divert around a full-extraction area in a seam above or below an active mining seam. The lateral extent of vertical stress increase is relatively narrow compared to the width of the full-extraction area. In addition, a zone of vertical stress relief occurs above and below the full-extraction area. It will extend to a distance up to the "critical width" of the extraction area. Horizontal stresses also divert around the full-extraction area; however, the distance that such stresses increase above or below the seam is much larger than the lateral extent of vertical stress increase. This distance may be approximately equal to the minimum width of the full-extraction area up to the "critical width." Thus, the size of this zone of vertical stress relief in conjunction with horizontal stress increase defines the

extent to which adverse multiple-seam mining interaction could occur.

Numerical modeling suggests four factors that control multiple-seam mining interactions and should be considered explicitly in design guidelines:

1. OB/IB thickness ratio;
2. Gob width-to-interburden thickness ratio;
3. Site-specific geology; and
4. Horizontal stress to rock strength ratio.

As mentioned earlier, the OB/IB ratio affects the geometry and the vertical stress level of the particular situation. Greater depth or closer proximity of the affected seam to undermining and overmining are both known to increase the chance of an interaction. The minimum gob width of the extraction area relative to the interburden thickness is another geometric factor that controls how far above or below a full-extraction area the horizontal stress might change. There are limits on this ratio that depend on whether the full-extraction area exceeds the "critical width" at which maximum subsidence is achieved and the vertical stress in the middle of the full-extraction area returns to its original in situ value. With respect to geology, the major variable is the percentage of strong rock in the interburden and where that strong rock is located relative to the affected roof. A suitably placed strong bed can shield the immediate roof rock of a seam from adverse multiple-seam mining interaction. Finally, the ratio of applied horizontal stress (in situ plus induced) to the strength of the immediate roof rock strength controls the degree of multiple-seam mining interaction. A higher ratio due to either high horizontal stress or low immediate roof rock strength increases the chance of an adverse interaction. Although horizontal stress has been found to be a major factor in many ground control problems, especially in the Eastern United States [Mark and Mucho 1994], the role of horizontal stress in multiple-seam mining interactions has received little attention in prior investigations.

REFERENCES

Chekan GJ, Listak JM [1993]. Design practices for multiple-seam longwall mines. Pittsburgh, PA: U.S. Department of the Interior, Bureau of Mines, IC 9360.

Chekan GJ, Listak JM [1994]. Design practices for multiple-seam room-and-pillar mines. Pittsburgh, PA: U.S. Department of the Interior, Bureau of Mines, IC 9403.

Dolinar DR [2003]. Variation of horizontal stresses and strains in mines in bedded deposits in the eastern and midwestern United States. In: Peng SS, Mark C, Khair AW, Heasley KA, eds. Proceedings of the 22nd International Conference on Ground Control in Mining. Morgantown, WV: West Virginia University, pp. 178–185.

Ellenberger JL, Chase FE, Mark C, Heasley KA, Marshall JK [2003]. Using site case histories of multiple-seam coal mining to advance mine design. In: Peng SS, Mark C, Khair AW, Heasley KA, eds. Proceedings of the 22nd International Conference on Ground Control in Mining. Morgantown, WV: West Virginia University, pp. 59–64.

Gale WJ [2004]. Rock fracture, caving and interaction of face supports under different geological environments: experience from Australian coal mines. In: Peng SS, Mark C, Finfinger GL, Tadolini SC, Heasley KA, Khair AW, eds. Proceedings of the 23rd International Conference on Ground Control in Mining. Morgantown, WV: West Virginia University, pp. 11–19.

Gale WJ, Tarrant GC [1997]. Let the rocks tell us. In: Doyle R, et al., eds. Symposium on Safety in Mines: The Role of Geology (Newcastle, New South Wales, Australia, November 24–25, 1997). Coalfield Geology Council of New South Wales, pp. 153–160.

Gale WJ, Mark C, Oyler DC, Chen J [2004]. Computer simulation of ground behavior and rock bolt interaction at Emerald mine. In: Peng SS, Mark C, Finfinger GL, Tadolini SC, Heasley KA, Khair AW, eds. Proceedings of the 23rd International Conference on Ground Control in Mining. Morgantown, WV: West Virginia University, pp. 27–34.

Haycocks C, Zhou Y [1990]. Multiple-seam mining: a state-of-the-art review. In: Proceedings of the Ninth International Conference on Ground Control in Mining. Morgantown, WV: West Virginia University, pp. 1–11.

Hill RW [1995]. Multiseam mining in South African Collieries. In: Peng SS, ed. Proceedings of the 14th International Conference on Ground Control in Mining. Morgantown, WV: West Virginia University, pp. 305–311.

Hladysz Z [1985]. Analysis of risk in multiple-seam mining. SME preprint 85–357. Littleton, CO: Society for Mining, Metallurgy, and Exploration, Inc.

Hsiung SM, Peng SS [1987a]. Design guidelines for multiple-seam mining, part I. Coal Min *24*(9):42–46.

Hsiung SM, Peng SS [1987b]. Design guidelines for multiple-seam mining, part II. Coal Min *24*(10):48–50.

Itasca Consulting Group [2000]. Fast Lagrangian analysis of continua. 2nd ed. Minneapolis, MN: Itasca Consulting Group, Inc.

Mark C, Mucho TP [1994]. Longwall mine design for control of horizontal stress. In: Mark C, Tuchman RJ, Repsher RC, Simon CL, eds. New Technology for Longwall Ground Control. Proceedings: U.S. Bureau of Mines Technology Transfer Seminar. Pittsburgh, PA: U.S. Department of the Interior, Bureau of Mines, SP 01–94, pp. 53–76.

Mark C, Molinda GM, Barton TM [2002]. New developments with the coal mine roof rating. In: Peng SS, Mark C, Khair AW, Heasley KA, eds. Proceedings of the 21st International Conference on Ground Control in Mining. Morgantown, WV: West Virginia University, pp. 294–301.

Molinda GM, Mark C [1996]. Rating the strength of coal mine roof rocks. Pittsburgh, PA: U.S. Department of the Interior, Bureau of Mines, IC 9444. NTIS No. PB96–155072.

Oyler DC, Mark C, Gale WJ, Chen J [2004]. Performance of roof support under high stress in a U.S. coal mine. SME preprint 04–135. Littleton, CO: Society for Mining, Metallurgy, and Exploration, Inc., pp. 1–9.

Rigsby KB, Jacobs D, Scovazzo VA [2003]. Design and experience of total extraction room-and-pillar operations above depleted longwall panels. In: Peng SS, Mark C, Khair AW, Heasley KA, eds. Proceedings of the 22nd International Conference on Ground Control in Mining. Morgantown, WV: West Virginia University, pp. 48–58.

This paper was previously published as:

Zipf RK Jr. [2005]. Failure mechanics of multiple-seam mining interactions. In: Peng SS, Mark C, Tadolini SC, Finfinger GL, Khair AW, Heasley KA, eds. Proceedings of the 24th International Conference on Ground Control in Mining. Morgantown, WV: West Virginia University, pp. 93–106.

CDC
Workplace Safety and Health

IC 9495

INFORMATION CIRCULAR/2007

Proceedings: New Technology for Ground Control in Multiple-seam Mining

Department of Health and Human Services
Centers for Disease Control and Prevention
National Institute for Occupational Safety and Health

NIOSH